



Study of the Weak Charged Hadronic Current in b Decays

M. Acciarri, O. Adriani, M. Aguilar-Benitez, S. Ahlen, B. Alpat, J. Alcaraz, G. Alemanni, J. Allaby, A. Aloisio, G. Alverson, et al.

► To cite this version:

M. Acciarri, O. Adriani, M. Aguilar-Benitez, S. Ahlen, B. Alpat, et al.. Study of the Weak Charged Hadronic Current in b Decays. Physics Letters B, 1997, 393, pp.477-486. 10.1016/S0370-2693(96)01689-9 . in2p3-00000258

HAL Id: in2p3-00000258

<https://hal.in2p3.fr/in2p3-00000258>

Submitted on 24 Nov 1998

HAL is a multi-disciplinary open access archive for the deposit and dissemination of scientific research documents, whether they are published or not. The documents may come from teaching and research institutions in France or abroad, or from public or private research centers.

L'archive ouverte pluridisciplinaire **HAL**, est destinée au dépôt et à la diffusion de documents scientifiques de niveau recherche, publiés ou non, émanant des établissements d'enseignement et de recherche français ou étrangers, des laboratoires publics ou privés.

Study of the Weak Charged Hadronic Current in b Decays

The L3 Collaboration

Abstract

Charged and neutral particle multiplicities of jets associated with identified semileptonic and hadronic b decays are studied. The observed differences between these jets are used to determine the inclusive properties of the weak charged hadronic current. The average charged particle multiplicity of the weak charged hadronic current in b decays is measured for the first time to be $2.69 \pm 0.07(\text{stat.}) \pm 0.14(\text{syst.})$. This result is in good agreement with the JETSET hadronization model of the weak charged hadronic current if $40 \pm 17\%$ of the produced mesons are light-flavored tensor ($L=1$) mesons. This level of tensor meson production is consistent with the measurement of the π^0 multiplicity in the weak charged hadronic current in b decays.

Submitted to *Physics Letters B*

1 Introduction

The decays of b hadrons are often described with the spectator model [1], where a b quark is assumed to decay into a charm quark and a virtual W boson. The basic weak decay dynamics of b hadrons are thus assumed to be similar to the decay properties of μ and τ leptons. The observed momentum spectra of the charged leptons [2], the neutrinos and thus the polarisation of the virtual W [3] in semileptonic b decays ($b \rightarrow c\ell\nu$) are well described by this model. Furthermore, the good agreement of the individual lifetimes of the different b mesons [4] indicates that the spectator model provides also a good approximation of hadronic b decays. Much less is known about purely hadronic b decays ($b \rightarrow c\bar{u}d$ and $b \rightarrow c\bar{s}s$) which have a branching ratio of more than 76%.

Measurements of inclusive hadron production in b decays exist [4], but their interpretation is in general difficult as these hadrons can be produced either directly or in the subsequent decays of the charmed hadron system. For the few identified decays a considerable fraction of tensor mesons ($L=1$) has been observed [5]. In contrast to hadronic b decays a multitude of measurements have been performed on the properties of the weak charged hadronic current (“the hadronic W^* current”) in semileptonic τ decays ($\tau \rightarrow \nu + \text{hadrons}$) [4]. Experimental information about the hadronic W^* current at the higher q^2 in b and c decays might lead to future theoretical insights into the weak decay dynamics of b and c flavored hadrons.

Assuming the spectator model ansatz, it is possible to extract some simple properties of the hadronic W^* current in b hadron decays. With this assumption, properties like the associated hadron multiplicities are essentially independent from the charm system in the b decay. Furthermore, in hadronic Z decays to $b\bar{b}$ jets the decay products from the two b hadrons are usually well separated from each other and the hadrons which are associated to the jet fragmentation and the cascade c hadron decays are similar for the jets containing semileptonic and hadronic b decays. Thus, the differences between the jets associated with semileptonic and hadronic b decays are related to the properties of the hadronic W^* current in b hadron decays. Such a comparison of jets which contain semileptonic and hadronic b decay candidates using the L3 detector is described in the following.

The L3 detector consists of a central tracking chamber, a high-resolution electro-magnetic calorimeter composed of BGO crystals, a cylindrical array of scintillation counters, a uranium and brass hadron calorimeter with proportional wire chamber readout, and a precise muon spectrometer. These detectors are installed in a 12 m diameter solenoid which provides a uniform field of 0.5 T along the beam direction. A detailed description of the L3 detector can be found elsewhere [6].

More than a million hadronic Z decays collected between 1991 and 1993, corresponding to an integrated luminosity of 46 pb^{-1} , are preselected using the criteria described in [7]. In order to reduce complications due to hard-gluon radiation, the measurements are performed using a selection of well measured two-jet events as explained in [8]. With these selection criteria 575k hadronic events are selected in the data and 450k events in the Monte Carlo sample. The hadronic Monte Carlo events are simulated using JETSET 7.3 [9] and a GEANT-based description of the L3 experiment [10].

The Monte Carlo simulation of the semileptonic b hadron decays is based on the results

discussed in [8], where a semileptonic branching ratio of 10.85% is used. Furthermore, the momentum spectrum of the weakly decaying b hadrons is simulated with the Peterson fragmentation function [11] as implemented in JETSET, with an average x_E of 0.72 as required by the observed momentum spectrum of electrons and muons in the two-jet event sample.

2 Selection of b-flavored jet samples

The selection of b-flavored jets with inclusive electrons and muons is identical to the ones used for our recent measurement of the semileptonic branching ratio ($b \rightarrow \ell \nu X$) [8]. High p and p_\perp electron and muon candidates are used to select b-flavored events and jets which contain semileptonic b decay candidates.

Electron candidates with a minimum energy of 3 GeV are selected in the barrel BGO calorimeter for the polar angle θ satisfying $|\cos \theta| < 0.72$. To separate electrons from other particles it is required that the lateral shower shape of the BGO clusters is consistent with that of an electromagnetic shower and that the centroid of this cluster is well matched in azimuthal angle with a charged track.

Muons are identified and measured in the muon chamber system by reconstructing a track with segments in at least two of the three detection layers. The muon track should point back to within 4σ of the interaction point in transverse and longitudinal distance of closest approach. The momentum of the track, corrected for the energy loss in the calorimeter, must be between 4 GeV and 35 GeV.

In order to select semileptonic b hadron decays among the electron and muon candidates, a p_\perp of more than 1.4 GeV with respect to the jet direction, excluding the charged lepton, is required.

With this selection 7561 jets with an electron candidate are selected. The purity for jets with correctly identified semileptonic b decays using this selection is found to be $78.7 \pm 2.1\%$. About 15% of the selected events originate from background of light-flavored jets and semileptonic charm decays. The sample of jets with inclusive muon candidates consists of 13967 jets with a purity of correctly identified semileptonic b decays of $69.6 \pm 1.3\%$ [8] and a background from light-flavored jets and semileptonic charm decays of 21%. Further details are found in [8].

Events which contain an inclusive lepton define the sample of $b\bar{b}$ events. In order to compare jets with semileptonic and hadronic b decays each event is divided into two hemispheres, defined by a plane perpendicular to the thrust axis. The particles associated to the hemisphere which contain the charged lepton define the semileptonic b decay jet sample. Particles in the hemisphere opposite to a hemisphere containing an inclusive lepton are assumed to originate from jets with a hadronic b decay. Assuming that all non semileptonic b decays are hadronic decays, one finds that about 65%(60%) of the jets opposite to the jet with the inclusive electron (muon) candidate contain the decay products of hadronic b decays. The fraction of jets with hadronic b decays can be enhanced with a removal of jets which have large missing energy due to energetic neutrinos from semileptonic b decays. With the requirement of a visible energy of more than 40 GeV for the jets opposite to the tagged jet, the fraction of jets which contain

hadronic b decays is found to be $75.4 \pm 1.2\%$ for the electron tagged events and $70.2 \pm 0.8\%$ for the muon tagged events. The number of jets selected as hadronic b-decay candidates are 5203 (9528) for electron (muon) tagged events.

3 Characteristics of the hadronic W^* current in b decays

We now compare the inclusive characteristics of jets which contain semileptonic and hadronic b hadron decays. From this analysis the average charged multiplicity, the associated inclusive momentum spectrum and the π^0 and η content of the hadronic W^* current are extracted.

3.1 The charged multiplicity of the hadronic W^* current

The tracks used for this analysis are required to be well measured and to have a minimum p_t of 100 MeV with respect to the beam direction. The main criteria for well-measured tracks are a minimum track length of 12.5 cm with reconstructed wire signals from at least 75% of the possible signals. Furthermore, the tracks should have a maximum distance of closest approach to the interaction point of 30 mm in the plane transverse to the beam and of 100 mm along the beam direction. After adjusting the Monte Carlo to describe the observed angular distributions of tracks for the different data taking periods the average tracking efficiency with these selection criteria is determined to be about 89%.

The track-multiplicity distributions of jets which contain identified leptons, excluding the lepton track, and for the jets with hadronic b decays, are shown in figure 1 (a) and (b) for electron- and muon-tagged events respectively. For the mean charged multiplicity a clear difference of about 2 tracks, between jets associated to hadronic and semileptonic b decay candidates is observed. The charged multiplicity for both kinds of jets, corrected for the tracking efficiency for the electron- and muon-tagged events in the data and in the Monte Carlo, are given in table 1.

The Monte Carlo is corrected by reweighting the tracking efficiency for each half-sector based on the measured tracking efficiency. The procedure gives good agreement between data and Monte Carlo for this efficiency as a function of the azimuthal angle. Conservatively the remaining difference between data and Monte Carlo is assumed to originate from the efficiency uncertainty and a systematic error of $\pm 3\%$ is assigned to the average tracking efficiency of 89% obtained from the Monte Carlo. This error covers also possible differences for the efficiency of jets with semileptonic and hadronic b hadron decays which are found to be smaller than 1%.

The charged multiplicity of the selected b decay hemispheres is 3–4% higher in the data than in the Monte Carlo sample. A similar difference is observed for the two jet hadronic event sample, where the average track multiplicity in the data is about 2% higher than in the Monte Carlo sample. This discrepancy could be related to the Monte Carlo description of the jet fragmentation or to an inaccurate simulation of the tracking efficiency. As the multiplicity of the charged hadronic current is obtained from the difference in the data between jets with

a semileptonic b decay and jets with a hadronic b decay, only the uncertainty from tracking efficiency is relevant for this measurement.

event type	lepton side -1 track			hadron side		
	data	MC	$P_{b \rightarrow l}$	data	MC	$P_{b \rightarrow \text{had}}$
electron $p_{\perp} > 1.4$ GeV	7.58 ± 0.04	7.20 ± 0.04	0.79	9.57 ± 0.05	9.32 ± 0.05	0.75
muon $p_{\perp} > 1.4$ GeV	7.61 ± 0.03	7.37 ± 0.03	0.70	9.64 ± 0.04	9.25 ± 0.04	0.70

Table 1: Observed average charge multiplicity of jets (tracking efficiency corrected) in the data and in the Monte Carlo for electron- and muon-tagged b flavored events. For jets which contain the lepton candidate one track is subtracted. The purities for semileptonic b decay jets ($P_{b \rightarrow l}$) and for correctly identified hadronic b decay jets ($P_{b \rightarrow \text{had}}$) are also given.

The multiplicity difference between jets containing hadronic and semileptonic b decays, $\Delta \langle n_{ch} \rangle$, must be corrected for background from light-flavored Z decays and wrongly identified b decays. The correction is derived from Monte Carlo adjusted to properly reproduce the charged lepton spectra and the semileptonic b hadron branching ratios [8]. The correction to $\Delta \langle n_{ch} \rangle$ is 0.47 ± 0.08 tracks for electron tagged events and 0.79 ± 0.07 tracks for muon tagged events.

The selection of semileptonic b decays with high p and p_{\perp} leptons favors jets with a slightly lower multiplicity. This bias was studied using a Monte Carlo sample containing only b decays and found to be 0.10 ± 0.07 tracks for electron tagged events and 0.10 ± 0.06 tracks for muon tagged events. These factors are added to the measured multiplicities of the hemispheres containing leptons. The systematic error of this correction was taken from the statistical error of the Monte Carlo. The 40 GeV minimum visible jet energy requirement was also studied and found to result in a negligible bias. Uncertainties from c and b decays, including D, D^* and D^{**} production were also found to be small.

The charged multiplicity measurement is further corrected for the contributions from weak decays of strange particles. The correction due to decays of such particles (mainly $K_S^0 \rightarrow \pi^+ \pi^-$) reduces the average multiplicity by 0.09 ± 0.01 . The systematic error due to this correction is included in the efficiency error given in table 2.

The changes from the uncorrected multiplicity difference between jets with hadronic and semileptonic b decays to the final result for the hadronic W^* current for electron- and muon-tagged events and the corresponding estimated contributions to the systematic error are summarised in table 2.

The average charged multiplicity for the electron tagged events is 2.5σ (statistical error only) lower than the one for the muon tagged events. A possible source of this discrepancy could be related to an inaccurate background description in the Monte Carlo for the fragmentation of light-flavored jets. No statistically significant source for this difference has been identified from a variation of the electron and muon selection criteria. However, it is found that a stronger cut against gluon radiation, e.g. removing events which have a hemisphere with an invariant mass larger than 15 GeV instead of 25 GeV, gives a more consistent results for the hadronic W^* multiplicity of 2.60 ± 0.13 and 2.74 ± 0.11 for the electron- and the muon-tagged events

type	data electrons	data muons
uncorrected $\Delta < n_{ch} >$	1.99 ± 0.07	2.03 ± 0.05
background and bias corrected	2.56 ± 0.11	2.92 ± 0.09
result (K_s^0 corr.)	2.47 ± 0.11	2.83 ± 0.09
systematic errors		
tracking efficiency (0.89 ± 0.03)	0.08	0.09
b,c decay systematics	0.04	0.04
MC $b \rightarrow \ell \nu X$ stat. (bias corr.)	0.07	0.06
b decay purity error	0.08	0.07
“two jet” definition	0.13	0.09
total error	0.19	0.16

Table 2: The difference for the charged track multiplicity for jets with semileptonic (the track from the lepton is subtracted) and hadronic b decays for electron- and muon-tagged events. The estimated contributions to the systematic errors are also given.

respectively. The difference between the result given in table 2 and the one with the jet mass cut of 15 GeV is added to the systematic error. The different contributions to the systematic error for the multiplicity measurement are also listed in table 2. While the uncertainties from the simulation of c and b hadron decays and the uncertainties in the tracking efficiency are correlated for the electron- and muon-tagged events, the errors related to the background corrections, the b purity, the bias of the method (estimated for 100% b purity) and the definition of the “two-jet” system are essentially independent for the two tagging methods.

Averaging electron- and muon-tagged events we obtain $\mathbf{2.69 \pm 0.07(stat.) \pm 0.14(syst.)}$ for the charged multiplicity of the hadronic W^* current in b hadron decays.

The comparison of jets associated to semileptonic and hadronic b hadron decays can also be used to study the momentum spectrum of charged particles associated to the weak charged hadronic current, using the scaled momentum $x_p = \frac{p}{E_{beam}}$. For this study the electron and muon events are combined. Figure 2 (a) and (b) show the observed x_p spectra in the data and simulation of all charged particles in jets associated to leptonic and hadronic b decays. Correcting each x_p bin using the procedure described above the x_p spectrum of the W^* is obtained. The data show a slightly harder x_p spectrum than the Monte Carlo. The systematic errors are found to be of the order of $\pm 10\%$ for x_p below 0.20. For larger momenta the errors are dominated by the limited Monte Carlo statistics.

3.2 The π^0 and η content of the hadronic W^* current

The π^0 and η content of semileptonic and hadronic b decays has also been studied. The two photon decays are used to reconstruct π^0 and η signals in the selected b event sample. The selection criteria are similar to those described in [12]. The π^0 's are selected in the momentum range between 0.4 to 3 GeV (η 's between 2 to 10 GeV).

After subtraction of the combinatorial background, 5112 ± 108 π^0 's are selected in jets with semileptonic b decays and 3107 ± 82 π^0 's in jets with hadronic b decays. The corresponding numbers of reconstructed η 's are 88 ± 15 in jets with semileptonic b decays and 45 ± 11 in jets with hadronic b decays.

To extract the π^0 and η content related to the hadronic W^* current the signals have to be corrected for the detection efficiency. Due to the lower multiplicity in semileptonic b decays one finds that the efficiency is up to a factor of two higher in jets with semileptonic b decays than for jets with hadronic b decays. After the corrections for background from light-flavored events and wrongly identified b jets, 1.80 ± 0.04 π^0 's are associated to jets with semileptonic b decays and 2.31 ± 0.07 for jets with hadronic b decays. The difference between the two type of jets is 0.51 ± 0.08 π^0 's. Finally, after applying the bias correction of 0.12 ± 0.09 , the π^0 multiplicity of the W^* current in the x_p range given above is measured to be **$0.63 \pm 0.09(\text{stat.}) \pm 0.11(\text{syst.})$** .

The measurement of the associated η multiplicity is limited by statistics. After applying the same corrections as for the π^0 's the number of η 's, with a momentum between 2 and 10 GeV, associated to the hadronic W^* current is found to be **$0.11 \pm 0.08(\text{stat.}) \pm 0.10(\text{syst.})$** .

4 Discussion of the results

The combined result of $2.69 \pm 0.07(\text{stat.}) \pm 0.14(\text{syst.})$ charged particles, associated to the hadronic W^* current in b hadron decays can be compared with the charged particle multiplicity in semileptonic τ decays, with an average of 1.455 ± 0.013 charged hadrons in the case of the τ lepton [4]. Such an increase is expected due to the higher mass¹⁾ of the virtual W in b hadron decays.

In a more quantitative analysis our results can be compared with expectations from JETSET 7.4 [13] with a fragmentation of the $W \rightarrow q\bar{q}$ system. Using the default parametrisation one finds on average 3.04 charged particles in the weak charged hadronic current. This is 2.2 standard deviations higher than in the data. The Monte Carlo multiplicity is found to be essentially identical for the W^* decay into $\bar{u}d$ and into $\bar{c}s$ quarks. However, the charged multiplicity for the $q\bar{q}$ system can be lowered if the production of tensor mesons (angular momentum $L=1$, spin $S=0,1$) is allowed. As shown in figure 3, the model provides good agreement with the data if $40 \pm 17\%$ of the produced hadrons are tensor mesons. As can also be seen from figure 3, the production rate of vector mesons with respect to pseudoscalar mesons is less important for the charged hadron multiplicity. A similar trend is found for the inclusive π^0 multiplicity where the number of π^0 's decreases from 0.83 for the default parametrisation to 0.75 for 40% tensor meson production. The measured π^0 multiplicity of $0.63 \pm 0.09(\text{stat.}) \pm 0.11(\text{syst.})$ is thus in good agreement with the tendency observed for charged particles.

It is worth pointing out that a large rate of tensor meson production in hadronic b decays can be expected as tensor mesons are also observed in the hadronic W^* current in τ and charm decays [4]. Furthermore, the observed fractions of resonant multi-pion states with respect to

¹⁾From a Monte Carlo study of b decays one finds an average mass of the hadronic system recoiling against the charmed hadron of about 2.3 GeV, compared to about 0.9 GeV for τ decays.

all observed multi-pion states in exclusive measurements of weak b hadron decays [5] indicate also a large fraction of tensor mesons.

The momentum spectrum of charged particles associated to the hadronic W^* current is shown in figure 4 for the data and the JETSET simulation adjusted to the production of 40% tensor mesons. The shape of the spectrum is found to be rather insensitive to the level of tensor meson production. The data indicate a slightly different hadron momentum spectrum than obtained from the Monte Carlo.

5 Summary

The structure of jets associated to hadronic and semileptonic b hadron decays has been studied. From the comparison of jets with associated semileptonic and hadronic b decays the average charge multiplicity of the hadronic W^* current in b decays and the momentum spectrum of the associated charged particles has been measured for the first time. The average charged hadron multiplicity, associated to the hadronic W^* current is found to be $2.69 \pm 0.07(\text{stat.}) \pm 0.14(\text{syst.})$. This is about one unit higher than the multiplicity of the hadronic W^* current in τ decays. The π^0 multiplicity is $0.63 \pm 0.09(\text{stat.}) \pm 0.10(\text{syst.})$ for π^0 's with a momentum between 0.4 and 3 GeV and the η multiplicity is $0.11 \pm 0.08(\text{stat.}) \pm 0.10(\text{syst.})$ for η 's between 2 and 10 GeV.

The data are in good agreement with the JETSET 7.4 phase space simulation of weak hadronic b decays if a fraction of $40 \pm 17\%$ tensor mesons is produced in the fragmentation of the hadronic W^* current. This result is consistent with the measured π^0 multiplicity. However, the momentum spectrum of the charged particles associated to the hadronic W^* current is not simultaneously described by the Monte Carlo.

Acknowledgments

We wish to express our gratitude to the CERN accelerator divisions for the excellent performance of the LEP machine. We acknowledge the contributions of all the engineers and technicians who have participated in the construction and maintenance of this experiment. Those of us who are not from member states thank CERN for its hospitality and help.

References

- [1] G. Altarelli, N. Cabibbo, G. Corbo, L. Maiani and G. Martinelli, Nucl. Phys. **B208** (1982) 365.
- [2] CLEO Collaboration, B. Barish *et al.*, Phys. Rev. Lett. **76** (1996) 1570.
- [3] L3 Collaboration, M. Acciarri *et al.*, Phys. Lett. **B351** (1995) 375.
- [4] Particle Data Group, R.M. Barnett *et al.*, Phys. Rev. **D54** (1996) 1.
- [5] CLEO Collaboration, D. Bortoletto *et al.*, Phys. Rev. **D45** (1992) 21.
- [6] L3 Collaboration, M. Adeva *et al.*, Nucl. Instr. Meth. **A289** (1990) 35.
- [7] L3 Collaboration, B. Adeva *et al.*, Z. Phys. **C51** (1991) 179.
- [8] L3 Collaboration, M. Acciarri *et al.*, Z. Phys. **C71** (1996) 379.
- [9] T. Sjöstrand, Computer Phys. Commun. **27** (1982) 243; and PYTHIA 5.6 and JETSET 7.3, CERN preprint CERN-TH 6488/92. More details about the simulation of c- and b-hadrons can be found in [3].
- [10] The L3 detector simulation is based on GEANT Version 3.14; see R. Brun *et al.*, GEANT 3, CERN/DD/EE/84-1 (Revised), September 1987 and GHEISHA program (H. Fesefeldt, RWTH Aachen Report PITHA 85/02 (1985) for the simulation of hadronic interactions.)
- [11] C. Peterson *et al.*, Phys. Rev. **D27** (1983) 105.
- [12] L3 Collaboration, M. Acciarri *et al.*, Phys. Lett. **B328** (1994) 223.
- [13] T. Sjöstrand, Computer Phys. Commun. **82** (1994) 74.

The L3 Collaboration:

M. Acciarri,²⁸ O. Adriani,¹⁷ M. Aguilar-Benitez,²⁷ S. Ahlen,¹¹ B. Alpat,³⁵ J. Alcaraz,²⁷ G. Alemanni,²³ J. Allaby,¹⁸ A. Aloisio,³⁰ G. Alverson,¹² M. G. Alvigi,³⁰ G. Ambrosi,²⁰ H. Anderhub,⁵⁰ V. P. Andreev,³⁹ T. Angelescu,¹³ F. Anselmo,⁹ D. Antreasyan,⁹ A. Arefiev,²⁹ T. Azemoon,³ T. Aziz,¹⁰ P. Bagnaia,³⁸ L. Baksay,⁴⁵ R. C. Ball,³ S. Banerjee,¹⁰ K. Banicz,⁴⁷ R. Barillere,¹⁸ L. Barone,³⁸ P. Bartalini,³⁵ A. Baschirotto,²⁸ M. Basile,⁹ R. Battiston,³⁵ A. Bay,²³ F. Becattini,¹⁷ U. Becker,¹⁶ F. Behner,⁵⁰ J. Berdugo,²⁷ P. Berges,¹⁶ B. Bertucci,¹⁸ B. L. Betev,⁵⁰ S. Bhattacharya,¹⁰ M. Biasini,¹⁸ A. Biland,⁵⁰ G. M. Bilei,³⁵ J. J. Blaising,¹⁸ S. C. Blyth,³⁶ G. J. Bobbink,² R. Bock,¹ A. Böhm,¹ B. Borgia,³⁸ A. Boucham,⁴ D. Bourilkov,⁵⁰ M. Bourquin,²⁰ D. Boutigny,⁴ J. G. Branson,⁴¹ V. Brigljevic,⁵⁰ I. C. Brock,³⁶ A. Buffini,¹⁷ A. Buijs,⁴⁶ J. D. Burger,¹⁶ W. J. Burger,²⁰ J. Busenitz,⁴⁵ A. Buytenhuijs,³² X. D. Cai,¹⁶ M. Campanelli,⁵⁰ M. Capell,¹⁶ G. Cara Romeo,⁹ M. Caria,³⁵ G. Carlino,⁴ A. M. Cartacci,¹⁷ J. Casaus,²⁷ G. Castellini,¹⁷ F. Cavallari,³⁸ N. Cavallo,³⁰ C. Cecchi,²⁰ M. Cerrada,²⁷ F. Cesaroni,²⁴ M. Chamizo,²⁷ A. Chan,⁵² Y. H. Chang,⁵² U. K. Chaturvedi,¹⁹ M. Chemarin,²⁶ A. Chen,⁵² G. Chen,⁷ G. M. Chen,⁷ H. F. Chen,²¹ H. S. Chen,⁷ M. Chen,¹⁶ G. Chiefari,³⁰ C. Y. Chien,⁵ M. T. Choi,⁴⁴ L. Cifarelli,⁴⁰ F. Cindolo,⁹ C. Civinini,¹⁷ I. Clare,¹⁶ R. Clare,¹⁶ H. O. Cohn,³³ G. Coignet,⁴ A. P. Colijn,² N. Colino,²⁷ V. Commichau,³ S. Costantini,³⁸ F. Cotorobai,¹³ B. de la Cruz,²⁷ A. Csilling,¹⁴ T. S. Dai,¹⁶ R. D'Alessandro,¹⁷ R. de Asmundis,³⁰ H. De Boeck,³² A. Degre,⁴ K. Deiters,⁴⁸ P. Denes,³⁷ F. DeNotaristefani,³⁸ D. DiBitonto,⁴⁵ M. Diemoz,³⁸ D. van Dierendonck,² F. Di Lodovico,⁵⁰ C. Dionisi,³⁸ M. Dittmar,⁵⁰ A. Dominguez,⁴¹ A. Doria,³⁰ I. Dorne,⁴ M. T. Dova,^{19,2} E. Drago,³⁰ D. Duchesneau,⁴ P. Duinker,² I. Duran,⁴² S. Dutta,¹⁰ S. Easo,³⁵ Yu. Efremenko,³³ H. El Mamouni,²⁶ A. Engler,³⁶ F. J. Eppling,¹⁶ F. C. Erne,² J. P. Ernenwein,²⁶ P. Extermann,²⁰ M. Fabre,⁴⁸ R. Faccini,³⁸ S. Falciano,³⁸ A. Favara,¹⁷ J. Fay,²⁶ O. Fedin,³⁹ M. Felcini,⁵⁰ B. Fenyi,⁴⁵ T. Ferguson,³⁶ D. Fernandez,²⁷ F. Ferroni,³⁸ H. Fesefeldt,¹ E. Fiandrini,³⁵ J. H. Field,²⁰ F. Filthaut,³⁶ P. H. Fisher,¹⁶ G. Forconi,¹⁶ L. Fredj,²⁰ K. Freudenreich,⁵⁰ C. Furetta,²⁸ Yu. Galaktionov,^{29,16} S. N. Ganguli,¹⁰ P. Garcia-Abia,²⁷ S. S. Gau,¹² S. Gentile,³⁸ J. Gerald,⁵ N. Gheordanescu,¹³ S. Giagu,³⁸ S. Goldfarb,²³ J. Goldstein,¹¹ Z. F. Gong,²¹ A. Gougas,⁵ G. Gratta,³⁴ M. W. Gruenewald,³ V. K. Gupta,³⁷ A. Gurtu,¹⁰ L. J. Gutay,⁴⁷ B. Hartmann,¹ A. Hasan,³¹ D. Hatzifotiadiou,⁹ T. Hebbeker,⁸ A. Hervé,¹⁸ W. C. van Hoek,³² H. Hofer,⁵⁰ H. Hoorani,²⁰ S. R. Hou,⁵² G. Hu,⁵ V. Innocenti,¹⁸ H. Janssen,⁴ K. Jenkes,¹ B. N. Jin,⁷ L. W. Jones,³ P. de Jong,¹⁸ I. Josa-Mutuberria,²⁷ A. Kasser,²³ R. A. Khan,¹⁹ D. Kamrad,⁴⁹ Yu. Kamyshev,³³ J. S. Kapustinsky,²⁵ Y. Karyotakis,⁴ M. Kaur,^{19,4} M. N. Kienzle-Focacci,²⁰ D. Kim,⁵ J. K. Kim,⁴⁴ S. C. Kim,⁴⁴ Y. G. Kim,⁴⁴ W. W. Kinnison,²⁵ A. Kirkby,³⁴ D. Kirkby,³⁴ J. Kirkby,¹⁸ D. Kiss,¹⁴ W. Kittel,³² A. Klimentov,^{16,29} A. C. König,³² I. Korolko,²⁹ V. Koutsenko,^{16,29} R. W. Kraemer,³⁶ W. Krenz,¹ H. Kuijten,³² A. Kunin,^{16,29} P. Ladron de Guevara,²⁷ G. Landi,¹⁷ C. Lapoint,¹⁶ K. Lassila-Perini,⁵⁰ P. Laurikainen,²² M. Lebeau,¹⁸ A. Lebedev,¹⁶ P. Lebrun,²⁶ P. Lecomte,⁵⁰ P. Lecoq,¹⁸ P. Le Coultre,⁵⁰ J. S. Lee,⁴⁴ K. Y. Lee,⁴⁴ C. Leggett,³ J. M. Le Goff,¹⁸ R. Leiste,⁴⁹ E. Leonardi,³⁸ P. Levchenko,³ C. Li,²¹ E. Lieb,⁴⁹ W. T. Lin,⁵² F. L. Linde,^{2,18} L. Lista,³⁰ Z. A. Liu,⁷ W. Lohmann,⁴⁹ E. Longo,³⁸ W. Lu,³⁴ Y. S. Lu,⁷ K. Lübelmeyer,¹ C. Luci,³⁸ D. Luckey,¹⁶ L. Luminari,³⁸ W. Lustermann,⁴⁸ W. G. Ma,²¹ M. Maity,¹⁰ G. Majumder,¹⁰ L. Malgeri,¹ A. Malinin,²⁹ C. Mañá,²⁷ S. Mangla,¹⁰ P. Marchesini,⁵⁰ A. Marin,¹¹ J. P. Martin,²⁶ F. Marzano,³⁸ G. G. G. Massaro,² D. McNally,¹⁸ S. Mele,³⁰ L. Merola,³⁰ M. Meschini,⁷ W. J. Metzger,³² M. von der Mey,¹ Y. Mi,²³ A. Mihul,¹³ A. J. W. van Mil,³² G. Mirabelli,³⁸ J. Mnich,¹⁸ P. Molnar,⁸ B. Monteleoni,¹⁷ R. Moore,³ S. Morganti,³⁸ T. Moulik,¹⁰ R. Mount,³⁴ S. Müller,¹ F. Muheim,²⁰ E. Nagy,¹⁴ S. Nahn,¹⁶ M. Napolitano,³⁰ F. Nessi-Tedaldi,⁵⁰ H. Newman,³⁴ T. Niessen,¹ A. Nippe,¹ A. Nisati,³⁸ H. Nowak,⁴⁹ H. Opitz,¹ G. Organtini,³⁸ R. Ostonen,²² D. Pandoulas,¹ S. Paoletti,³⁸ P. Paolucci,³⁰ H. K. Park,³⁶ G. Pascale,³⁸ G. Passaleva,¹⁷ S. Patricelli,³⁰ T. Paul,¹² M. Pauluzzi,³⁵ C. Paus,¹ F. Pauss,⁵⁰ D. Peach,¹⁸ Y. J. Pei,¹ S. Pensotti,²⁸ D. Perret-Gallix,⁴ S. Petrak,⁸ A. Pevsner,⁵ D. Piccolo,³⁰ M. Pieri,¹⁷ J. C. Pinto,³⁶ P. A. Piroué,³⁷ E. Pistolesi,²⁸ V. Plyaskin,²⁹ M. Pohl,⁵⁰ V. Pojidaev,^{29,17} H. Postema,¹⁶ N. Produit,²⁰ D. Prokofiev,³⁹ G. Rahal-Callot,⁵⁰ P. G. Rancoita,²⁸ M. Rattaggi,²⁸ G. Raven,⁴¹ P. Razis,³¹ K. Read,³³ D. Ren,⁵⁰ M. Rescigno,³⁸ S. Reucroft,¹² T. van Rhee,⁴ S. Riemann,⁴⁹ B. C. Riemers,⁴⁷ K. Riles,³ O. Rind,³ S. Ro,⁴⁴ A. Robohn,⁵⁰ J. Rodin,¹⁶ F. J. Rodriguez,²⁷ B. P. Roe,³ L. Romero,²⁷ S. Rosier-Lees,⁴ Ph. Rosselet,²³ W. van Rossum,⁴⁶ S. Roth,¹ J. A. Rubio,¹⁸ H. Rykaczewski,⁵⁰ J. Salicio,¹⁸ E. Sanchez,²⁷ A. Santocchia,³⁵ M. E. Sarakinos,²² S. Sarkar,¹⁰ M. Sassowsky,¹ G. Sauvage,⁴ C. Schäfer,¹ V. Schegelsky,³⁹ S. Schmidt-Kaerst,¹ D. Schmitz,¹ P. Schmitz,¹ M. Schneegans,⁴ N. Scholz,⁵⁰ H. Schopper,⁵¹ D. J. Schotanus,³² J. Schwenke,¹ G. Schwering,¹ C. Sciacca,³⁰ D. Sciarrino,²⁰ J. C. Sens,⁵² L. Servoli,³⁵ S. Shevchenko,³⁴ N. Shivarov,⁴³ V. Shoutko,²⁹ J. Shukla,²⁵ E. Shumilov,²⁹ A. Shvorob,³⁴ T. Siedenburt,¹ D. Son,⁴⁴ A. Sopczak,⁴⁹ V. Soulimov,³⁰ B. Smith,¹⁶ P. Spillantini,¹⁷ M. Steuer,¹⁶ D. P. Stickland,³⁷ H. Stone,³⁷ B. Stoyanov,⁴³ A. Straessner,¹ K. Strauch,¹⁵ K. Sudhakar,¹⁰ G. Sultanov,¹⁹ L. Z. Sun,²¹ G. F. Susinno,²⁰ H. Suter,⁵⁰ J. D. Swain,¹⁹ X. W. Tang,⁷ L. Tauscher,⁶ L. Taylor,¹² Samuel C. C. Ting,¹⁶ S. M. Ting,¹⁶ M. Tonutti,¹ S. C. Tonwar,¹⁰ J. Tóth,¹⁴ C. Tully,³⁷ H. Tuchscherer,⁴⁵ K. L. Tung,⁷ Y. Uchida,¹⁶ J. Ulbricht,⁵⁰ U. Uwer,¹⁸ E. Valente,³⁸ R. T. Van de Walle,³² G. Vesztegombi,¹⁴ I. Vetlitsky,²⁹ G. Viertel,⁵⁰ M. Vivargent,⁴ R. Völkert,⁴⁹ H. Vogel,³⁶ H. Vogt,⁴⁹ I. Vorobiev,²⁹ A. A. Vorobyov,³⁹ A. Vorvolakos,³¹ M. Wadhwa,⁵ W. Wallraff,¹ J. C. Wang,¹⁶ X. L. Wang,²¹ Z. M. Wang,²¹ A. Weber,¹ F. Wittgenstein,¹⁸ S. X. Wu,¹⁹ S. Wynhoff,¹ J. Xu,¹¹ Z. Z. Xu,²¹ B. Z. Yang,²¹ C. G. Yang,⁷ X. Y. Yao,⁷ J. B. Ye,²¹ S. C. Yeh,⁵² J. M. You,³⁶ An. Zalite,³⁹ Yu. Zalite,³⁹ P. Zemp,⁵⁰ Y. Zeng,¹ Z. Zhang,⁷ Z. P. Zhang,²¹ B. Zhou,¹¹ Y. Zhou,³ G. Y. Zhu,⁷ R. Y. Zhu,³⁴ A. Zichichi,^{9,18,19} F. Ziegler.⁴⁹

- 1 I. Physikalisches Institut, RWTH, D-52056 Aachen, FRG[§]
 - III. Physikalisches Institut, RWTH, D-52056 Aachen, FRG[§]
 - 2 National Institute for High Energy Physics, NIKHEF, and University of Amsterdam, NL-1009 DB Amsterdam, The Netherlands
 - 3 University of Michigan, Ann Arbor, MI 48109, USA
 - 4 Laboratoire d'Annecy-le-Vieux de Physique des Particules, LAPP, IN2P3-CNRS, BP 110, F-74941 Annecy-le-Vieux CEDEX, France
 - 5 Johns Hopkins University, Baltimore, MD 21218, USA
 - 6 Institute of Physics, University of Basel, CH-4056 Basel, Switzerland
 - 7 Institute of High Energy Physics, IHEP, 100039 Beijing, China[△]
 - 8 Humboldt University, D-10099 Berlin, FRG[§]
 - 9 INFN-Sezione di Bologna, I-40126 Bologna, Italy
 - 10 Tata Institute of Fundamental Research, Bombay 400 005, India
 - 11 Boston University, Boston, MA 02215, USA
 - 12 Northeastern University, Boston, MA 02115, USA
 - 13 Institute of Atomic Physics and University of Bucharest, R-76900 Bucharest, Romania
 - 14 Central Research Institute for Physics of the Hungarian Academy of Sciences, H-1525 Budapest 114, Hungary[‡]
 - 15 Harvard University, Cambridge, MA 02139, USA
 - 16 Massachusetts Institute of Technology, Cambridge, MA 02139, USA
 - 17 INFN Sezione di Firenze and University of Florence, I-50125 Florence, Italy
 - 18 European Laboratory for Particle Physics, CERN, CH-1211 Geneva 23, Switzerland
 - 19 World Laboratory, FBLJA Project, CH-1211 Geneva 23, Switzerland
 - 20 University of Geneva, CH-1211 Geneva 4, Switzerland
 - 21 Chinese University of Science and Technology, USTC, Hefei, Anhui 230 029, China[△]
 - 22 SEFT, Research Institute for High Energy Physics, P.O. Box 9, SF-00014 Helsinki, Finland
 - 23 University of Lausanne, CH-1015 Lausanne, Switzerland
 - 24 INFN-Sezione di Lecce and Università Degli Studi di Lecce, I-73100 Lecce, Italy
 - 25 Los Alamos National Laboratory, Los Alamos, NM 87544, USA
 - 26 Institut de Physique Nucléaire de Lyon, IN2P3-CNRS, Université Claude Bernard, F-69622 Villeurbanne, France
 - 27 Centro de Investigaciones Energeticas, Medioambientales y Tecnologicas, CIEMAT, E-28040 Madrid, Spain^b
 - 28 INFN-Sezione di Milano, I-20133 Milan, Italy
 - 29 Institute of Theoretical and Experimental Physics, ITEP, Moscow, Russia
 - 30 INFN-Sezione di Napoli and University of Naples, I-80125 Naples, Italy
 - 31 Department of Natural Sciences, University of Cyprus, Nicosia, Cyprus
 - 32 University of Nymegen and NIKHEF, NL-6525 ED Nymegen, The Netherlands
 - 33 Oak Ridge National Laboratory, Oak Ridge, TN 37831, USA
 - 34 California Institute of Technology, Pasadena, CA 91125, USA
 - 35 INFN-Sezione di Perugia and Università Degli Studi di Perugia, I-06100 Perugia, Italy
 - 36 Carnegie Mellon University, Pittsburgh, PA 15213, USA
 - 37 Princeton University, Princeton, NJ 08544, USA
 - 38 INFN-Sezione di Roma and University of Rome, "La Sapienza", I-00185 Rome, Italy
 - 39 Nuclear Physics Institute, St. Petersburg, Russia
 - 40 University and INFN, Salerno, I-84100 Salerno, Italy
 - 41 University of California, San Diego, CA 92093, USA
 - 42 Dept. de Fisica de Particulas Elementales, Univ. de Santiago, E-15706 Santiago de Compostela, Spain
 - 43 Bulgarian Academy of Sciences, Central Laboratory of Mechatronics and Instrumentation, BU-1113 Sofia, Bulgaria
 - 44 Center for High Energy Physics, Korea Advanced Inst. of Sciences and Technology, 305-701 Taejon, Republic of Korea
 - 45 University of Alabama, Tuscaloosa, AL 35486, USA
 - 46 Utrecht University and NIKHEF, NL-3584 CB Utrecht, The Netherlands
 - 47 Purdue University, West Lafayette, IN 47907, USA
 - 48 Paul Scherrer Institut, PSI, CH-5232 Villigen, Switzerland
 - 49 DESY-Institut für Hochenergiephysik, D-15738 Zeuthen, FRG
 - 50 Eidgenössische Technische Hochschule, ETH Zürich, CH-8093 Zürich, Switzerland
 - 51 University of Hamburg, D-22761 Hamburg, FRG
 - 52 High Energy Physics Group, Taiwan, China
- [§] Supported by the German Bundesministerium für Bildung, Wissenschaft, Forschung und Technologie
[‡] Supported by the Hungarian OTKA fund under contract number T14459.
^b Supported also by the Comisión Interministerial de Ciencia y Tecnología
[‡] Also supported by CONICET and Universidad Nacional de La Plata, CC 67, 1900 La Plata, Argentina
[◇] Also supported by Panjab University, Chandigarh-160014, India
[△] Supported by the National Natural Science Foundation of China.

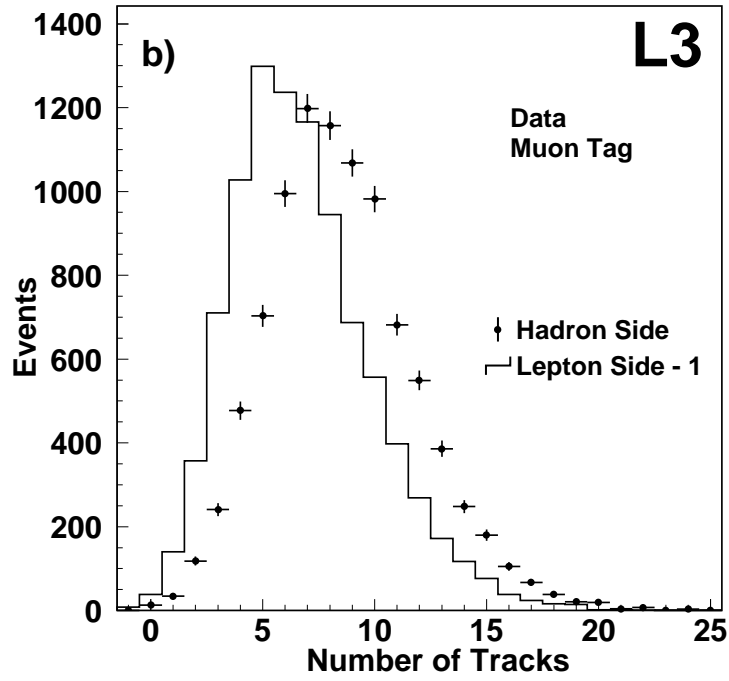
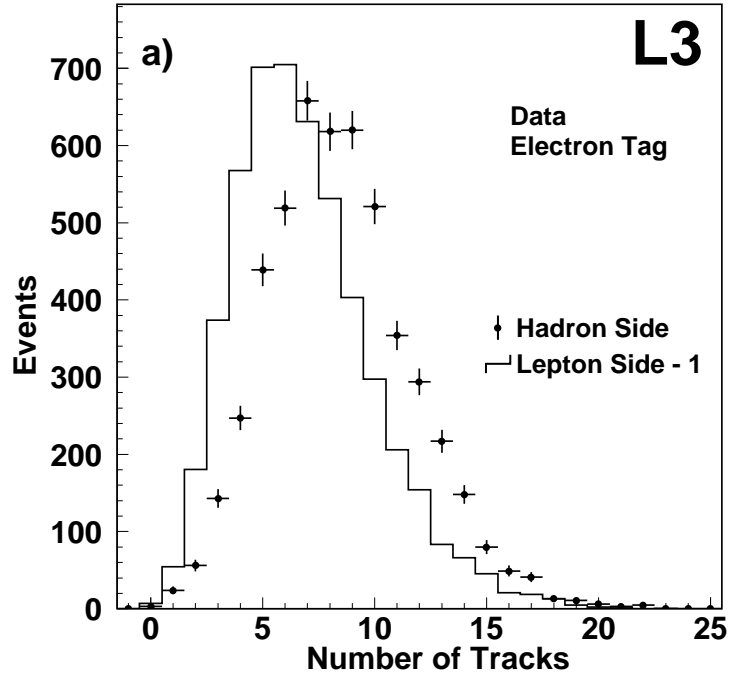


Figure 1: Comparison of the measured charged multiplicity for the lepton side (the lepton is subtracted) and the hadron side in the data, (a) is for electron-tagged events and (b) for muon-tagged events.

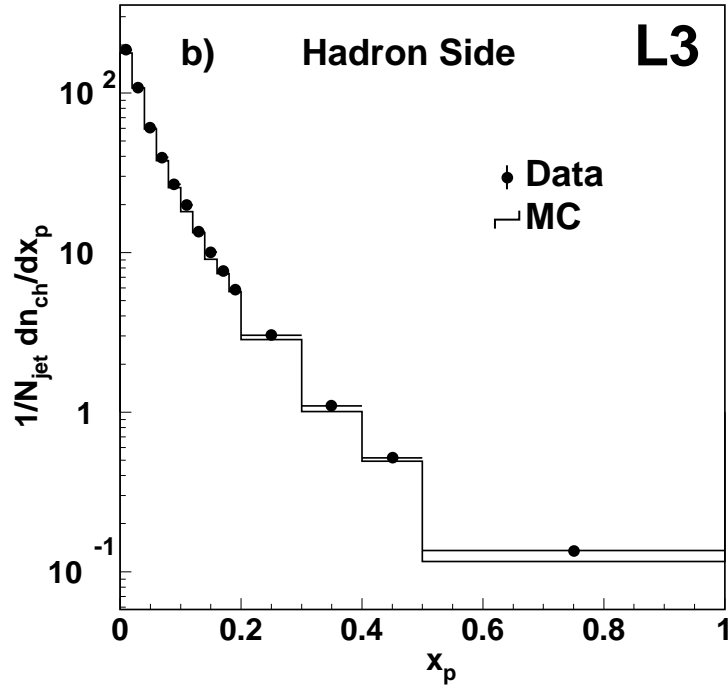
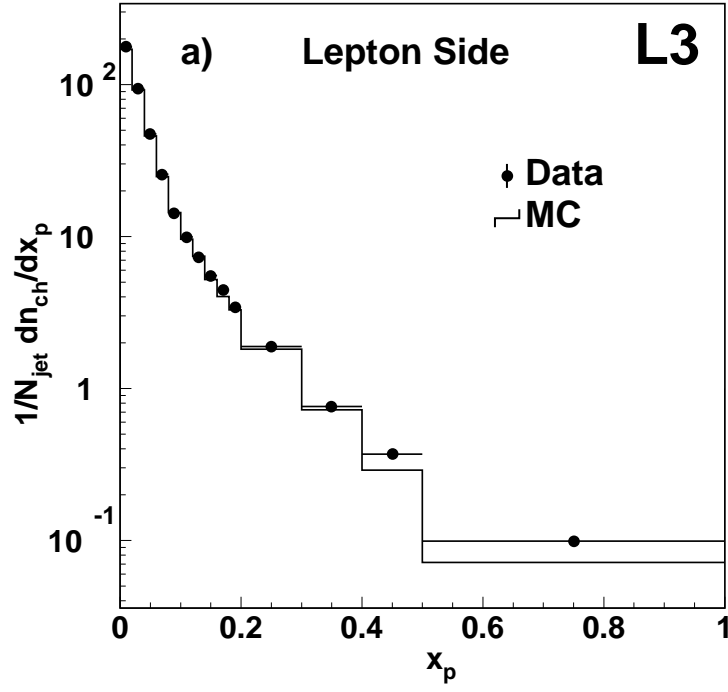


Figure 2: The observed momentum spectrum x_p for charged particles in the data and the Monte Carlo for jets which contain the lepton (a) and for jets opposite to the lepton with a visible energy above 40 GeV (b).

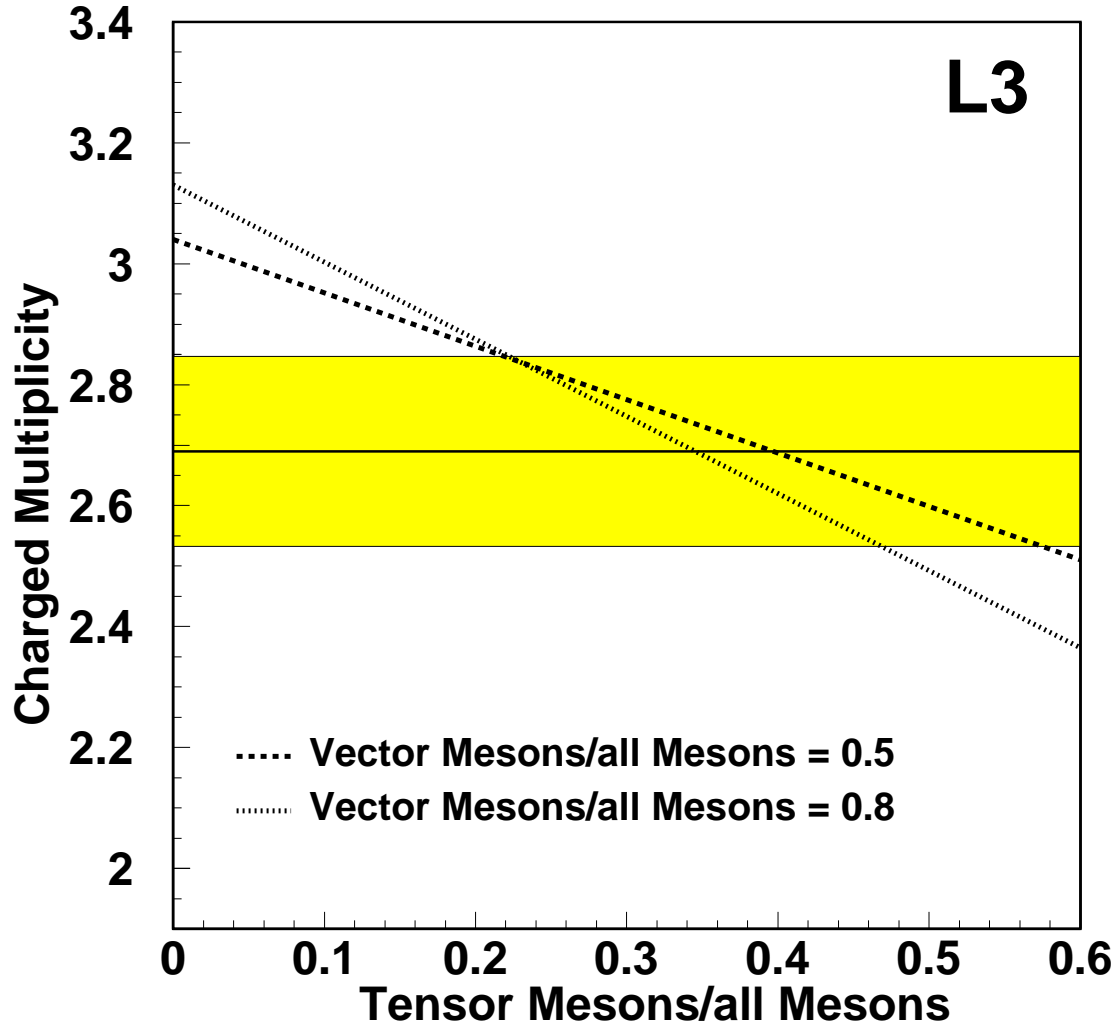


Figure 3: Comparison of the charged multiplicity of the W^* in the data and the JETSET 7.4 fragmentation model. The horizontal band shows the allowed range from the measurement. The two dashed lines show the multiplicity prediction as a function of the tensor mesons production rate for two different production rates of vector mesons.

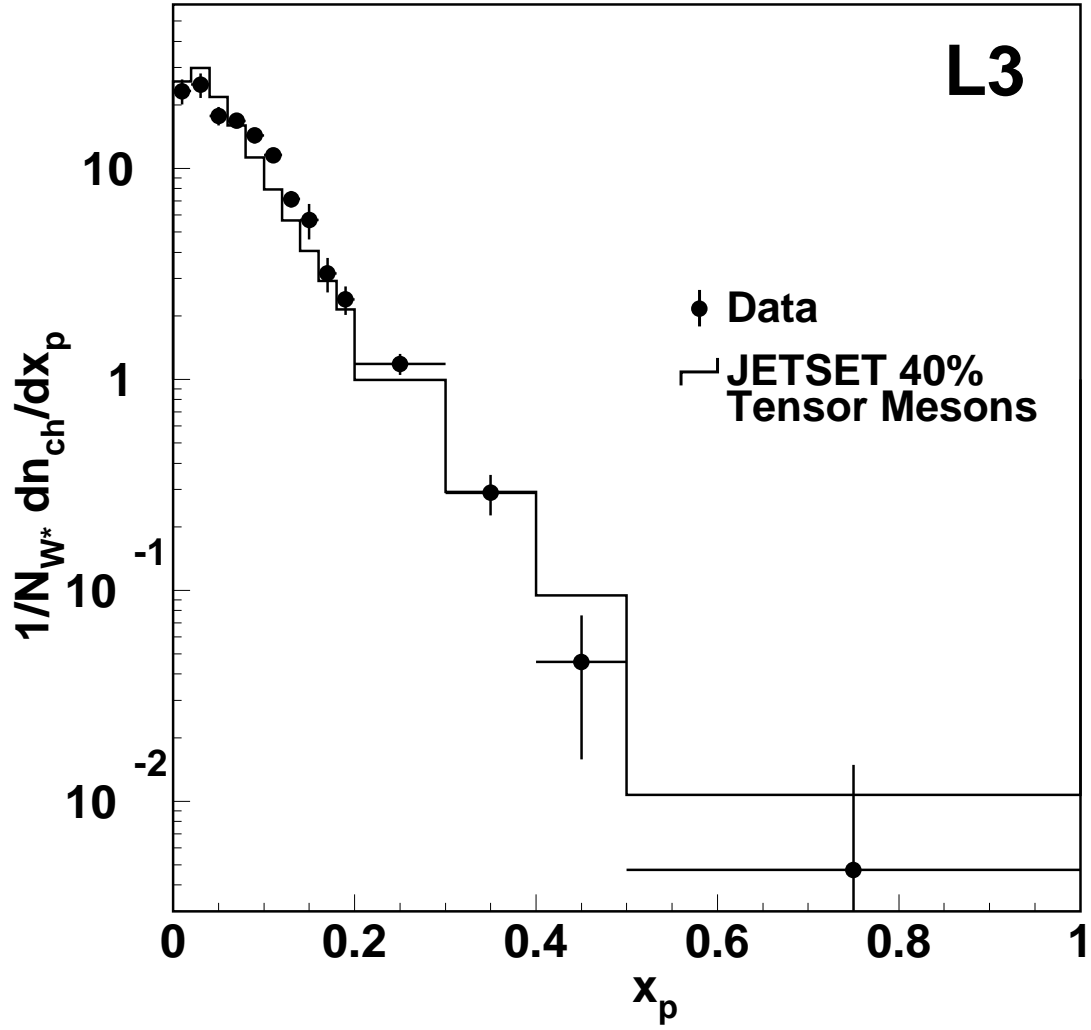


Figure 4: Comparison of the measured momentum spectrum of the charged hadrons associated to the weak charged current in the data and the JETSET 7.4 fragmentation model with 40% tensor meson production probability.